Pulsed inductively coupled chlorine plasmas in the presence of a substrate bias

Pramod Subramonium[a)]
Department of Chemical Engineering, University of Illinois, 1406 West Green Street, Urbana, Illinois 61801

Mark J. Kushner[b)]
Department of Electrical and Computer Engineering, University of Illinois, 1406 West Green Street, Urbana, Illinois 61801

(Received 6 June 2001; accepted for publication 24 July 2001)

Pulsed inductively coupled plasmas (ICPs) sustained in electronegative gas mixtures using a substrate bias are being investigated to achieve improved etching characteristics in microelectronics fabrication. Experiments have shown that electron temperatures in pulsed ICPs without a substrate bias monotonically decrease during the afterglow. Under select conditions with a substrate bias, electron temperatures increase in the late afterglow. These trends suggest a transition in power deposition from inductive to capacitive. To investigate these processes, a two-dimensional, computationally parallel model was developed for pulsed ICPs. Results for Cl_2 plasmas indicate that with a substrate bias the sheath thickness and speed, and hence electron heating, increase during the afterglow as the electron density decays. When the sheath reaches a critical thickness, capacitive electron heating begins. © *2001 American Institute of Physics.* [DOI: 10.1063/1.1406139]

High plasma density sources are widely used to define fine features in microelectronics fabrication.[1,2] As device sizes continue to decrease, undesirable characteristics such as notching become more pronounced.[3] Notching, thought to be due to differential charging in features, may be alleviated if negative ions can be injected into the feature to neutralize charge deposited by positive ions. Experiments have shown that pulsed electronegative plasmas may perform this function.[3–5] Many previous studies have addressed pulsed inductively coupled plasmas (ICPs) in the absence of substrate biases and found that the plasma transitions from an electron–ion to an ion–ion plasma commensurate with a decay in the plasma potential and electron temperature during the afterglow.[4,6,7] This transition bodes well for being able to extract negative ions, however, the use of a substrate bias is additionally required to accelerate the negative ions into features. In this regard Malyshev and Donnely investigated pulsed ICPs in 10 mTorr Cl_2 at 300 W with a continuous radio frequency (rf) substrate bias.[4] They found that there was no significant difference in plasma characteristics with or without the rf bias during the ICP power-on period (activeglow). However, with a 12.5 MHz bias, during the ICP power-off period (afterglow) the electron temperature increased rapidly after having dropped in the early afterglow.

In this letter, results from our computational investigation of Cl_2 pulsed ICPs with and without a continuous rf substrate bias are presented. The results of our model qualitatively agree with the experiments by Malyshev and Donnely.[4] We found that the electron temperature drops in the early afterglow. However, as a result of a decreasing electron density, the sheath thickens thereby producing more electron heating. When the sheath exceeds a critical thickness and heating rate in the late afterglow, an increase in the electron temperature is then produced. The plasma properties in the activeglow with or without the substrate bias were similar.

A moderately parallel implementation of the Hybrid Plasma Equipment Model (HPEM) was used in this investigation.[8] The parallel model (HPEM-P) employs "task parallelism" using compiler directives provided in OPENMP (Ref. 9) to concurrently execute different modules of the HPEM on three processors of a symmetric multiprocessor computer having shared memory. The modules are: the Electromagnetics Module (EMM); the Electron Energy Transport Module (EETM); and the Fluid Kinetics Module (FKM). In doing so, parameters from the different modules can be exchanged on a frequent and, in some cases, arbitrarily specified basis without interrupting the time-evolving calculation being performed in any other module. For example, the plasma conductivity and electron collision frequency are continuously updated in the FKM. These parameters are available in shared memory where they are accessed by the EMM to produce nearly continuous updates of the electromagnetic fields. These fields are then made immediately available to the EETM through shared memory, along with parameters from the FKM, to update electron-impact source functions and transport coefficients. These parameters are then transferred to the FKM, again through shared memory, as they are updated to compute densities, fluxes, and electrostatic fields. The hierarchy captures long-term transients by directly interfacing short plasma time scales with long-term neutral time scales. The HPEM-P options we used are continuity, momentum, and energy equations for all neutral and ion species, a semi-implicit solution of Poisson's equation using a drift-diffusion formulation for electron continuity, and the Electron Monte Carlo Simulation of the EETM, which resolves the electron energy distributions in two dimensions as a function of time.

We investigated pulsed Cl_2 plasmas with and without a continuous rf substrate bias. The ICP reactor geometry,

[a)]Electronic mail: subramon@uiuc.edu
[b)]Electronic mail: mjk@uiuc.edu

0003-6951/2001/79(14)/2145/3/$18.00 © 2001 American Institute of Physics
Downloaded 05 Oct 2001 to 128.174.115.149. Redistribution subject to AIP license or copyright, see http://ojps.aip.org/aplo/aplcr.jsp

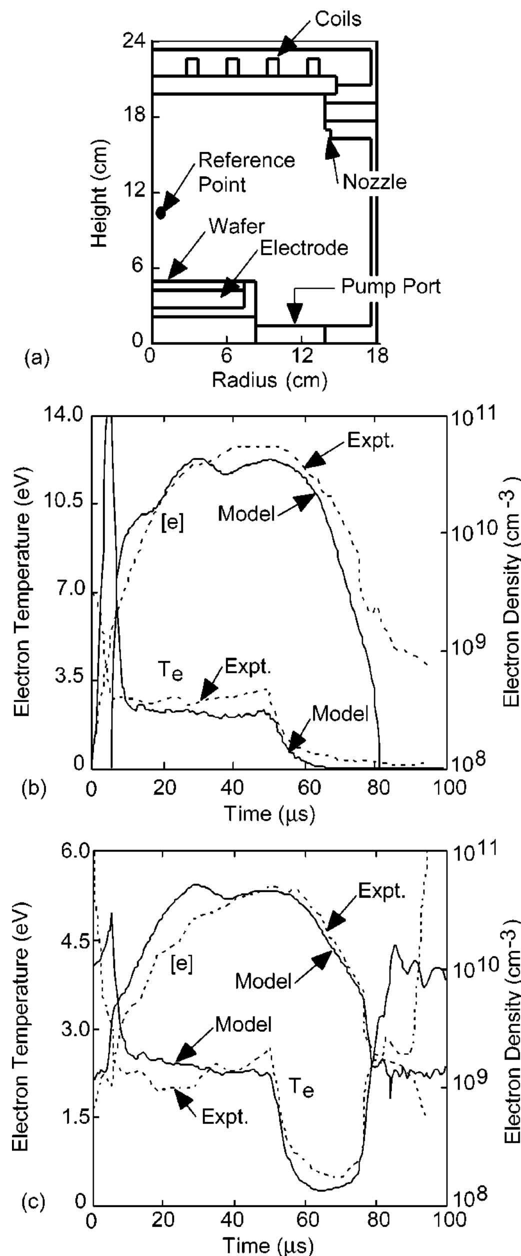

FIG. 1. Electron densities and temperature in Cl_2 plasmas at 10 mTorr with a time-averaged power of 300 W, PRF of 10 kHz, duty cycle of 50%, and gas flow rate of 100 sccm with and without substrate bias. (a) Schematic of the ICP reactor; (b) comparison of model predictions with measurements by Malyshev and Donnely (see Ref. 4) at the reference point shown in (a) without a substrate bias; and (c) electron density and temperature with a substrate bias (250 V).

shown in Fig. 1(a), is based on the experiments of Malyshev and Donnely.[4] The base case conditions are 10 mTorr, time-averaged ICP power of 300 W (peak power 600 W) at 10 MHz, continuous substrate bias of amplitude 250 V at 10 MHz (approximately 70 W time averaged), pulse repetition frequency (PRF) of 10 kHz, and duty cycle of 50%. The electron temperature (T_e) and density (n_e) as a function of time at the reference point without and with a substrate bias are shown in Fig. 1 compared to the results of Malyshev and Donnely.[4] The ramp-up in n_e during the activeglow is similar in both cases, reaching a maximum of $\approx 8\times10^{10}\,\mathrm{cm}^{-3}$ at the end of the power-on period (50 μs). Upon termination of the power, n_e rapidly decays, largely due to the decrease in ionization and increase in attachment to Cl_2, which accompanies the decrease in T_e. The decay in n_e is more rapid without the bias, a difference attributed to the more positive time-averaged plasma potential with the bias. The decay in n_e with a bias significantly slows with an increase in T_e late in the afterglow. If the afterglow is extended to a few 100 μs, n_e attains a quasisteady state corresponding to a capacitively coupled discharge.

T_e during the steady state of the activeglow is nearly the same, 2.5–3 eV, with or without the bias. When the ICP power is first turned on, T_e peaks in both cases, a consequence of power being deposited into the initially smaller inventory of electrons remaining at the end of the previous afterglow. A higher T_e is required for the smaller inventory of electrons to dissipate the desired power. The peak in T_e is ≈ 9 eV without the bias and 5 eV with the bias, a consequence of the smaller electron inventory at the end of the afterglow without a bias. During the first 25 μs of the afterglow, T_e monotonically decreases in both cases, a result of electron thermalization in the absence of ICP heating and diffusion cooling. During this time, the electron density is still sufficiently large, and sheath thickness sufficiently small, that sheath heating by the bias is not important. Therefore, there is little difference in T_e with or without the bias.

T_e in the late afterglow is quite different with and without the bias. Without the bias, T_e continues to fall until thermalizing with the gas, accompanied by a monotonic decrease in the plasma potential. After 25 μs into the afterglow with the bias, T_e begins to increase. Recall that sheath heating scales with the square of sheath speed v_s, the sheath thickness λ scales as $n_e^{-1/2}$ and $v_s \approx \omega\lambda$.[10] ($\omega$ is the bias frequency.) The total rate of sheath heating H, therefore, scales as $H \sim v_s^2 n_e$, which is then not a function of n_e. The specific heating rate (power per electron), h, scales as $H/n_e \sim 1/n_e$. Therefore, as n_e decays, primarily by dissociative attachment to Cl_2, sheath thickness λ increases, producing an increase in v_s and a net increase in specific heating rate h. This results in an increase in (or slowing in the rate of decrease of) T_e. When h is sufficiently large (n_e sufficiently small) in the late afterglow that sheath heating exceeds the rate of collisional loss, T_e increases. Results from the model for T_e and n_e are compared with the experiments by Malyshev and Donnely[4] in Fig. 1. The experimental trends are well captured.

T_e with a bias at different times during the power on-and-off cycle is shown in Fig. 2. After 4 μs into the activeglow T_e peaks near the coils with an extended skin depth due to the low initial electron density. At this early time, n_e is still sufficiently small, and λ sufficiently large, that sheath heating is still important and there is a second peak in T_e near the substrate. After 10 μs, n_e has started to increase, thereby reducing λ and h , and so T_e near the substrate decreases. T_e peaks only under the coil in a more confined region due to the shorter skin depth. At 45 μs in the late activeglow, the peak in T_e has decreased due to the larger n_e, which is able to dissipate the desired power at a lower temperature. T_e is also more uniform due to the higher thermal conductivity. Sheath heating at the substrate is negligible due to the high n_e and small λ. At 80 μs (35 μs into the afterglow), T_e is low throughout the reactor in the absence of ICP heating. n_e is still sufficiently large (and λ small) that

Downloaded 05 Oct 2001 to 128.174.115.149. Redistribution subject to AIP license or copyright, see http://ojps.aip.org/aplo/aplcr.jsp

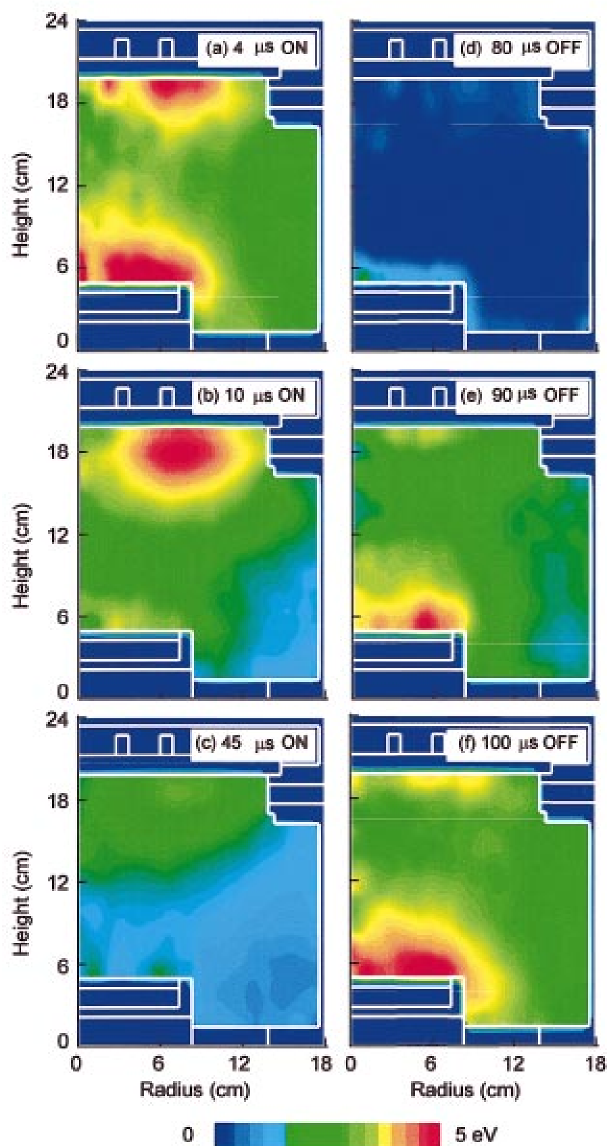

FIG. 2. (Color) Electron temperature in a Cl_2 plasma at different times for the conditions of Fig. 1 with a substrate bias. The power is turned off at 50 μs. Results are shown for (a) 4 μs, (b) 10 μs, and (c) 45 μs during the power-on period and (d) 80 μs, (e) 90 μs, and (f) 100 μs during the afterglow. Sheath heating occurs when the electron density falls below a critical value in the afterglow.

sheath heating does not dominate, although there is a small increase in T_e near the substrate. At 90 and 100 μs (the end of the afterglow), T_e becomes increasingly larger first near the substrate and later over much of the reactor as n_e approaches its minimum value and sheath heating is near its maximum. By 90 μs, the discharge has transitioned into a capacitively coupled mode.

The transition to a capacitive mode, as indicated by an increase in T_e during the afterglow, occurs when h is sufficiently large that it dominates over thermalization and inelastic losses. One would, therefore, expect the onset of the capacitive mode to occur at shorter times into the afterglow with increasing amplitude of the bias. This expectation is confirmed by the results in Fig. 3, which show the time for

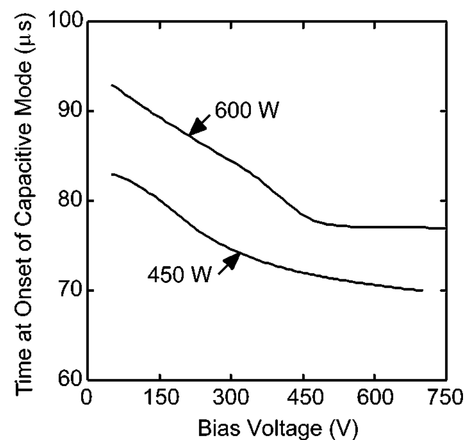

FIG. 3. The onset time for the capacitive mode, as indicated by a sharp increase in electron temperature, as a function of rf bias amplitude for ICP powers of 450 and 600 W. The ICP power is turned off at 50 μs.

onset of the capacitive mode as a function of bias voltage amplitude. (The afterglow begins at 50 μs.) Larger biases produce capacitive heating at shorter times. The afterglow is not long enough for the onset of the capacitive mode with biases less than 50 V. With a larger ICP power, n_e at the end of the activeglow is larger and the decay in the afterglow from attachment is smaller due to the larger degree of dissociation of Cl_2. As a consequence, the critical electron density and sheath thickness required to trigger the onset of the capacitive mode occurs later in the afterglow, as shown in Fig. 3.

One of the purposes of pulsed ICP sources with biases is to accelerate negative ions into features. The onset of the capacitive mode in large part prevents this from occurring due to the reestablishment of large positive plasma potentials. These results indicate that for a given set of operating conditions (e.g., power, pressure, gas mixture, PRF, duty cycle), there is a critical bias voltage (and frequency), above which a capacitive mode will be established during the afterglow. Operating below this critical value is necessary in order to optimally extract negative ions.

This work was supported by the National Science Foundation (Grant CTS99-74962) and the Semiconductor Research Corp.

[1] W. Collision, T. Q. Ni, and M. S. Barnes, J. Vac. Sci. Technol. A **16**, 100 (1998).
[2] J. Y. Choe, I. P. Herman, and V. M. Donnely, J. Vac. Sci. Technol. A **15**, 3024 (1997).
[3] S. Samukawa, K. Noguchi, K. H. A. Bogart, and M. V. Malyshev, J. Vac. Sci. Technol. B **18**, 834 (2000).
[4] M. V. Malyshev and V. M. Donnely, Plasma Sources Sci. Technol. **9**, 353 (2000).
[5] S. Kanakasabapathy, L. J. Overzet, V. Midha, and D. Economou, Appl. Phys. Lett. **78**, 22 (2001).
[6] G. A. Hebner and C. B. Fleddermann, J. Appl. Phys. **82**, 2814 (1997).
[7] M. V. Malyshev, V. M. Donnelly, J. I. Colonell, and S. Samukawa, J. Appl. Phys. **86**, 4813 (1999).
[8] R. L. Kinder and M. J. Kushner, J. Vac. Sci. Technol. A **19**, 76 (2001).
[9] Kuck and Associates, Inc., http://www.kai.com/parallel/kappro
[10] M. A. Lieberman and A. J. Lichtenberg, *Principles of Plasma Discharges and Materials Processing* (Wiley-Interscience, New York, 1994), Chap. 11.

Downloaded 05 Oct 2001 to 128.174.115.149. Redistribution subject to AIP license or copyright, see http://ojps.aip.org/aplo/aplcr.jsp